ЖЭТФ, 2016, том 149, вып. 4, стр. 770–785

DECAYS OF A NEUTRAL PARTICLE WITH ZERO SPIN AND ARBITRARY CP PARITY INTO TWO OFF-MASS-SHELL Z BOSONS

T. V. Zagoskin [a*], ***A. Yu. Korchin*** [a,b**]

[a] *NSC "Kharkov Institute of Physics and Technology" 61108, Kharkov, Ukraine*

[b] *V. N. Karazin Kharkov National University 61022, Kharkov, Ukraine*

Received May 16, 2015

We investigate effects of CP symmetry violation in the decay of a scalar particle X (the Higgs boson) into two off-mass-shell Z bosons both decaying into a fermion–antifermion pair, $X \to Z_1^* Z_2^* \to f_1\overline{f}_1 f_2\overline{f}_2$. The most general form of the amplitude of the transition $X \to Z_1^* Z_2^*$, wherein the boson X may not have definite CP parity, is considered. The applicability limits of the narrow-Z-width approximation used in obtaining differential widths of the decay under consideration are determined. Various observables connected with the structure of the amplitude of the decay $X \to Z_1^* Z_2^*$ are studied. These observables are analyzed in the Standard Model as well as in models conceding indefinite CP parity of the Higgs boson. An experimental measurement of angular and invariant mass distributions of the decay $X \to Z_1^* Z_2^* \to f_1\overline{f}_1 f_2\overline{f}_2$ at the LHC can give information about the CP properties of the Higgs boson and its interaction with the Z boson.

DOI: 10.7868/S0044451016040052

1. INTRODUCTION

In 2012, the ATLAS and CMS collaborations detected [1] a neutral boson h with a mass of about 126 GeV. Currently, detailed study of the properties of this particle, called the Higgs boson, is an important task. The Standard Model (SM) Higgs boson is a state with $J^{CP} = 0^{++}$, and all the available experimental data on the properties of the particle h are close to the corresponding theoretical predictions about the SM Higgs boson (see, e. g., [2–4]). In particular, the spin of the boson h is equal to zero or two, and many hypotheses in which the spin of h is two are excluded with probability 95 % or higher [3]. At the same time, the situation may be more complicated. For example, some supersymmetric models predict the existence of neutral bosons with negative or even indefinite CP parity [5–7].

The issue of the CP parity of the Higgs boson is also related to the search for CP symmetry breaking sources that are additional to the mechanism built into the Cabibbo–Kobayashi–Maskawa quark-mixing matrix. Such sources of CP violation, for example, in the Higgs sector, could help in explaining the known problem of the matter–antimatter asymmetry in the Universe [8].

It has been suggested [9, 10] that the CP properties of the Higgs boson be studied by investigating the decays into two photons, $h \to \gamma\gamma$, via measurement of the polarization characteristics of the photons. In Refs. [11], the decay to the photon and the Z boson, $h \to Z^*\gamma \to f\bar{f}\gamma$, has been examined, and in [12, 13], the decay to the photon and a lepton pair, $h \to \gamma l^+ l^-$, was studied. In these papers, it has been shown that the "forward–backward" asymmetry for the final fermions carries information about the CP properties of the h boson and physics beyond the SM.

Investigating the decay of the Higgs boson into two Z bosons with their consequent decay into fermions is another opportunity to ascertain the CP properties of h. Such a cascade decay wherein the final fermions are leptons, along with the two-photon decay channel, has allowed the determination [1] of the mass of the particle h with the highest accuracy. In Refs. [14–17], theoretical distributions of the decay $h \to Z_1^* Z_2^* \to f_1\bar{f}_1 f_2\bar{f}_2$ have been studied at various values of the spin of h

* E-mail: taras.zagoskin@gmail.com
** E-mail: korchin@kipt.kharkov.ua

and in the case of various CP properties of this boson. It was reported in [14] what properties of the experimental distributions testify about a particular spin and a particular CP parity of h. In [15–17], asymmetries whose measurement allows clarifying the mentioned properties of the Higgs boson are suggested and investigated. Finally, various methods for obtaining constraints on the Higgs boson couplings to ZZ, W^-W^+, $\gamma\gamma$, and $Z\gamma$ from experimental data were proposed in [18].

Besides, various theories with spontaneous breaking of conformal invariance (for example, theories of technicolor) assume the existence of one more neutral spin-zero particle interacting with the gauge bosons, the dilaton. At present, the mass of the dilaton is not determined, but according to the estimates in Ref. [19], the mass can exceed 10^4 GeV in some models. Along with that, it was shown in [20–22] that the variant in which the boson h is the dilaton is not excluded.

To clarify the CP properties of the particle h and the hypothetical dilaton, we consider a neutral particle X with zero spin and arbitrary CP parity. We examine the decay $X \to Z_1^* Z_2^* \to f_1\bar{f}_1 f_2\bar{f}_2$ in the case of the nonidentical fermions, $f_1 \neq f_2$, and study in detail the differential width of this decay with respect to the three angles of the fermions in the helicity frame and with respect to the invariant masses of the fermion pairs $f_1\bar{f}_1$ and $f_2\bar{f}_2$. The most general $X \to Z_1^* Z_2^*$ vertex, which generalizes the corresponding SM vertex and contains a term corresponding to the negative CP parity of the particle X, is used.

We also find the applicability limits of the narrow-width approximation for the Z boson for the presented calculation of differential widths of the above decay. By means of this approximation, we derive a formula for the total width of the decay $X \to Z_1^* Z_2^* \to f_1\bar{f}_1 f_2\bar{f}_2$ (the formula is also valid in the case $f_1 = f_2$) and a formula for the total width of the decay $h \to Z_1^* Z_2^*$. These formulas are more general and more precise than those obtained in Ref. [23].

Next we find observables connected with the structure of the amplitude of the decay $X \to Z_1^* Z_2^*$. The formula for the fully differential decay width contains 9 coefficients related to the amplitude $X \to Z_1^* Z_2^*$. For each of them, one or two observables linear in this coefficient are defined. We note that some of these observables, as well as different ones, have been studied in [15–17, 24], but we also obtain new experimentally measurable quantities and analyze the dependences of the observables on the mass of one of the Z bosons (Z_2^*) in much greater detail than it has been done in those papers. This analysis is carried out in the framework of the SM as well as in certain SM extensions where the boson h is a mixture of a CP-even state and a CP-odd one. Measurement of the suggested observables at the LHC can yield important information about the CP properties of the Higgs boson and its interaction with the Z boson.

2. FORMALISM FOR THE DECAYS $X \to Z_1^* Z_2^* \to f_1\overline{f}_1 f_2\overline{f}_2$

2.1. The amplitude of the decay $X \to Z_1^* Z_2^*$ and the fully differential decay width for $X \to Z_1^* Z_2^* \to f_1\overline{f}_1 f_2\overline{f}_2$

We consider the decay of a neutral spin-zero particle X with arbitrary CP parity into two off-mass-shell Z bosons (Z_1^* and Z_2^*), each of which decays into a fermion–antifermion pair, $f_1\bar{f}_1$ and $f_2\bar{f}_2$:

$$X \to Z_1^* Z_2^* \to f_1\bar{f}_1 f_2\bar{f}_2, \tag{1}$$

where $m_X > 2(m_{f_1} + m_{f_2})$ (to satisfy the energy conservation law in the rest frame of X), m_X is the mass of the particle X, and m_{f_j} is the mass of the fermion f_j. We consider this decay at the tree level. If $m_X \in (4m_b, 2m_t]$ (where m_b is the mass of the b quark and m_t is the mass of the t quark), which is the case if $X = h$, then $f_j = e^-, \mu^-, \tau^-, \nu_e, \nu_\mu, \nu_\tau, u, c, d, s, b$. If $m_X > 4m_t$, which is possible [19] if X is the dilaton, then f_j can also be the top quark.

From the energy–momentum conservation, we find that a_1 and a_2 (where a_j is the mass squared of the boson Z_j^*, i. e., the invariant mass squared of the pair $f_j\bar{f}_j$) lie within the limits

$$\begin{aligned} 4m_{f_1}^2 < a_1 < (m_X - 2m_{f_2})^2, \\ 4m_{f_2}^2 < a_2 < (m_X - \sqrt{a_1}\,)^2. \end{aligned} \tag{2}$$

The amplitude $A_{X\to Z_1^* Z_2^*}(\lambda_1, \lambda_2)$ of the decay of X into Z_1^* and Z_2^* is [15–17, 24]

$$\begin{aligned} A_{X\to Z_1^* Z_2^*}(\lambda_1, \lambda_2) = 2\sqrt{\sqrt{2}G_F}\, m_Z^2 \Big(a_Z (e_1^* \cdot e_2^*) + \\ + \frac{b_Z}{m_X^2}(e_1^* \cdot (p_1 + p_2))(e_2^* \cdot (p_1 + p_2)) + \\ + i\,\frac{c_Z}{m_X^2}\varepsilon_{\mu\nu\rho\sigma}(p_1^\mu + p_2^\mu)(p_1^\nu - p_2^\nu)(e_1^\rho)^*(e_2^\sigma)^* \Big), \end{aligned} \tag{3}$$

where λ_j, e_j, and p_j are respectively the helicity, the polarization 4-vector, and the 4-momentum of the boson Z_j^*, G_F is the Fermi constant, m_Z is the mass of the Z boson, a_Z, b_Z, and c_Z are complex-valued dimensionless functions of a_1 and a_2, and $\varepsilon_{\mu\nu\rho\sigma}$ is the Levi-Civita symbol ($\varepsilon_{0123} = 1$). We note that at the tree level,

— if X is the SM Higgs boson, then $a_Z = 1$ and $b_Z = c_Z = 0$;

— if the CP parity of X is -1, then $a_Z = b_Z = 0$ and $c_Z \neq 0$;

— if the CP parity of X is indefinite, then $a_Z \neq 0$, $c_Z \neq 0$ and/or $b_Z \neq 0$, $c_Z \neq 0$.

Calculating the Lorentz-invariant amplitude $A_{X\to Z_1^* Z_2^*}(\lambda_1, \lambda_2)$ in the reference frame in which $\mathbf{p}_1 + \mathbf{p}_2 = 0$, we derive that

$$
\begin{aligned}
&A_{X\to Z_1^* Z_2^*}(-1,-1) = 2\sqrt{\sqrt{2}G_F}m_Z^2 \times \\
&\qquad\times\left(a_Z - c_Z\frac{\lambda^{\frac{1}{2}}(m_X^2,a_1,a_2)}{m_X^2}\right), \\
&A_{X\to Z_1^* Z_2^*}(0,0) = -2\sqrt{\sqrt{2}G_F}m_Z^2 \times \\
&\quad\times\left(a_Z\frac{m_X^2-a_1-a_2}{2\sqrt{a_1a_2}} + b_Z\frac{\lambda(m_X^2,a_1,a_2)}{4m_X^2\sqrt{a_1a_2}}\right), \qquad (4)\\
&A_{X\to Z_1^* Z_2^*}(1,1) = 2\sqrt{\sqrt{2}G_F}m_Z^2 \times \\
&\qquad\times\left(a_Z + c_Z\frac{\lambda^{\frac{1}{2}}(m_X^2,a_1,a_2)}{m_X^2}\right), \\
&A_{X\to Z_1^* Z_2^*}(\lambda_1,\lambda_2) = 0, \quad \lambda_1 \neq \lambda_2,
\end{aligned}
$$

where the function $\lambda(x,y,z)$ is defined in the standard way:

$$\lambda(x,y,z) = x^2 + y^2 + z^2 - 2xy - 2xz - 2yz.$$

To describe decay (1), we introduce the following angles (see Fig. 1): θ_1 (θ_2) is the angle between the momentum of Z_1^* (Z_2^*) in the rest frame of X and the momentum of f_1 (f_2) in the rest frame of Z_1^* (Z_2^*), and φ is the azimuthal angle between the planes of the decays $Z_1^* \to f_1\bar{f}_1$ and $Z_2^* \to f_2\bar{f}_2$. In what follows, we discuss the case of the nonidentical fermions, $f_1 \neq f_2$.

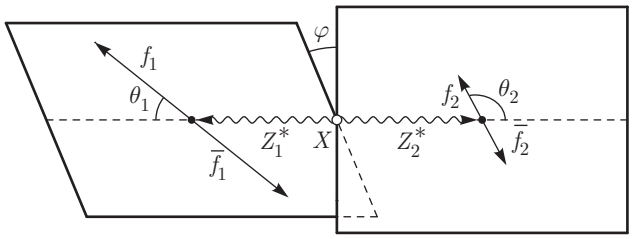

Fig. 1. The kinematics of the decay $X \to Z_1^* Z_2^* \to f_1\bar{f}_1 f_2\bar{f}_2$. The momenta of Z_1^* and Z_2^* are shown in the rest frame of X, and the momenta of f_1 and $\bar{f}_1$ (f_2 and $\bar{f}_2$) are shown in the rest frame of Z_1^* (Z_2^*)

Using the helicity formalism (see, e. g., [25]), we obtain that in the approximation of massless fermions, $m_{f_1} = m_{f_2} = 0$, the differential decay width of (1) with respect to a_1, a_2, θ_1, θ_2, φ has the form

$$
\begin{aligned}
&\frac{d^5\Gamma}{da_1 da_2 d\theta_1 d\theta_2 d\varphi} = \frac{\sqrt{2}G_F^3 m_Z^8}{(4\pi)^6 m_X^3}(a_{f_1}^2+v_{f_1}^2)(a_{f_2}^2+v_{f_2}^2)\times \\
&\times\frac{\lambda^{1/2}(m_X^2,a_1,a_2)a_1a_2}{D(a_1)D(a_2)}\sin\theta_1\sin\theta_2[(|A_\parallel|^2+|A_\perp|^2)\times \\
&\times\left((1+\cos^2\theta_1)(1+\cos^2\theta_2)+4A_{f_1}A_{f_2}\cos\theta_1\cos\theta_2\right)+ \\
&+4|A_0|^2\sin^2\theta_1\sin^2\theta_2 - 4\,\mathrm{Re}(A_\parallel^* A_\perp)\times \\
&\times(A_{f_1}\cos\theta_1(1+\cos^2\theta_2)+A_{f_2}\cos\theta_2(1+\cos^2\theta_1))+ \\
&+4\sqrt{2}\sin\theta_1\sin\theta_2((\mathrm{Re}(A_0^* A_\parallel)\cos\varphi - \\
&-\mathrm{Im}(A_0^* A_\perp)\sin\varphi)(A_{f_1}A_{f_2}+\cos\theta_1\cos\theta_2) - \\
&-(\mathrm{Re}(A_0^* A_\perp)\cos\varphi - \mathrm{Im}(A_0^* A_\parallel)\sin\varphi)\times \\
&\times(A_{f_1}\cos\theta_2 + A_{f_2}\cos\theta_1))+ \\
&+\sin^2\theta_1\sin^2\theta_2((|A_\parallel|^2-|A_\perp|^2)\cos 2\varphi - \\
&-2\,\mathrm{Im}(A_\parallel^* A_\perp)\sin 2\varphi)], \qquad (5)
\end{aligned}
$$

where a_f is the projection of the weak isospin of a fermion f,

$$v_f \equiv a_f - 2\frac{q_f}{e}\sin^2\theta_W,$$

q_f is the electric charge of a fermion f, e is the electric charge of the positron, θ_W is the weak mixing angle,

$$D(a_{1,2}) \equiv (a_{1,2} - m_Z^2)^2 + (m_Z\Gamma_Z)^2,$$

Γ_Z is the total width of the Z boson,

$$A_f \equiv \frac{2a_f v_f}{a_f^2 + v_f^2},$$

and

$$
\begin{aligned}
&A_\parallel(a_1,a_2) \equiv \\
&\equiv\frac{A_{X\to Z_1^* Z_2^*}(1,1)+A_{X\to Z_1^* Z_2^*}(-1,-1)}{2^{7/4}\sqrt{G_F}m_Z^2} = \sqrt{2}a_Z, \\
&A_\perp(a_1,a_2) \equiv \\
&\equiv\frac{A_{X\to Z_1^* Z_2^*}(1,1)-A_{X\to Z_1^* Z_2^*}(-1,-1)}{2^{7/4}\sqrt{G_F}m_Z^2} = \\
&\qquad = \sqrt{2}c_Z\frac{\lambda^{1/2}(m_X^2,a_1,a_2)}{m_X^2}, \qquad (6)\\
&A_0(a_1,a_2) \equiv \frac{A_{X\to Z_1^* Z_2^*}(0,0)}{2^{5/4}\sqrt{G_F}m_Z^2} = \\
&= -\left(a_Z\frac{m_X^2-a_1-a_2}{2\sqrt{a_1a_2}} + b_Z\frac{\lambda(m_X^2,a_1,a_2)}{4m_X^2\sqrt{a_1a_2}}\right).
\end{aligned}
$$

The approximation $m_{f_1} = m_{f_2} = 0$ is used in what follows. Using Eq. (5), we can connect the ratios of the quantities $|A_0|^2$, $|A_\parallel|^2 + |A_\perp|^2$, $|A_\parallel|^2 - |A_\perp|^2$, $\mathrm{Re}(A_0^* A_\parallel)$, $\mathrm{Im}(A_0^* A_\parallel)$, $\mathrm{Re}(A_0^* A_\perp)$, $\mathrm{Im}(A_0^* A_\perp)$,

$\mathrm{Re}(A_\parallel^* A_\perp)$, $\mathrm{Im}(A_\parallel^* A_\perp)$ to $|A_0|^2 + |A_\parallel|^2 + |A_\perp|^2$ with functions of a_1 and a_2 that can be measured in experiment. We call these ratios the helicity coefficients of the decay $X \to Z_1^* Z_2^*$.

2.2. The differential width $d^2\Gamma/da_1da_2$

The number of the decays

$$h \to Z_1^* Z_2^* \to l_1^- l_1^+ l_2^- l_2^+ \quad (l_j = e, \mu), \tag{7}$$

detected in the ATLAS experiment [2], where the invariant mass of the four leptons was in the interval [120 GeV, 130 GeV], is equal to 32. The number of decays (7) detected in the CMS experiment [3], in which the four-lepton invariant mass was in the range [121.5 GeV, 130.5 GeV], is equal to 25. In view of the insignificant amount of data, an experimental dependence of the distribution

$$\frac{1}{\Gamma}\frac{d^5\Gamma}{da_1 da_2 d\theta_1 d\theta_2 d\varphi}$$

(where Γ is the total width of decay (1)) for any of decays (7) is currently not available. We consider differential decay widths of (1) with respect to four and fewer variables. Integrating Eq. (5) with respect to θ_1, θ_2, φ, we obtain

$$\frac{d^2\Gamma}{da_1 da_2} = \frac{\sqrt{2}G_F^3 m_Z^8}{9(2\pi)^5 m_X^3}(a_{f_1}^2 + v_{f_1}^2)(a_{f_2}^2 + v_{f_2}^2)\times \\ \times \frac{\lambda^{1/2}(m_X^2, a_1, a_2)a_1 a_2}{D(a_1)D(a_2)} \sum_{p=0,\parallel,\perp} |A_p|^2. \tag{8}$$

It follows from Eqs. (8) and (6) that the dependence of the differential width $d^2\Gamma/da_1da_2$ on a_Z, b_Z, c_Z reduces to only the dependence on $|a_Z|$, $|b_Z|$, $|c_Z|$, and $\cos(\arg b_Z - \arg a_Z)$.

The available experimental data on the properties of the particle h are close to the corresponding theoretical predictions for the SM Higgs boson (see, e. g., [2–4]). That is why $a_{hZ} \approx 1$, $b_{hZ} \approx 0$, and $c_{hZ} \approx 0$, where

$$a_{hZ} \equiv a_Z|_{X=h}, \quad b_{hZ} \equiv b_Z|_{X=h}, \quad c_{hZ} \equiv c_Z|_{X=h}.$$

In Fig. 2, we show the differential decay width (8) for $X \to Z_1^* Z_2^* \to l_1^- l_1^+ l_2^- l_2^+$ ($l_j = e, \mu, \tau, l_1 \neq l_2$) as a function of $\sqrt{a_1}$ and $\sqrt{a_2}$ in the SM for $|a_Z| = 1$, $b_Z = c_Z = 0$, and $m_X = m_h$, where m_h is the mass of the Higgs boson h. The range of $\sqrt{a_1}$ and $\sqrt{a_2}$ in this plot is determined by inequalities (2) in the approximation of massless fermions. In calculations and in plotting graphs, the experimental data listed in Table 1 are used, and $\sin^2\theta_W = 1 - m_W^2/m_Z^2$, where m_W is the mass of the W boson.

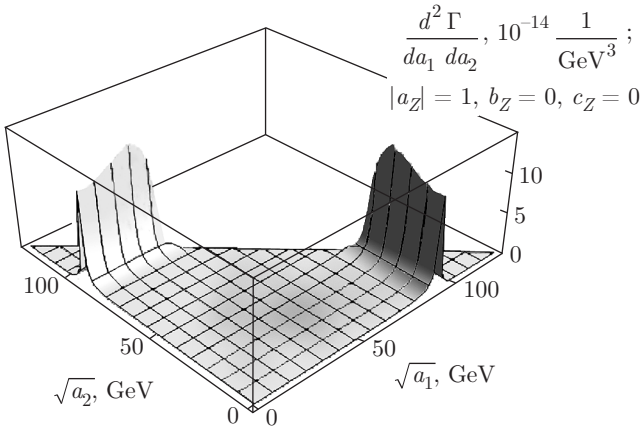

Fig. 2. The dependence of the differential decay width $d^2\Gamma/da_1da_2$ of $X \to Z_1^* Z_2^* \to l_1^- l_1^+ l_2^- l_2^+$ ($l_j = e, \mu, \tau$; $l_1 \neq l_2$) on $\sqrt{a_1}$ and $\sqrt{a_2}$ in the SM for $m_X = m_h$

Table 1. Values of the Fermi constant, of the masses of h, Z, and W, and of the total width of Z [26]

$G_F = 1.1663787(6) \cdot 10^{-5}$ GeV^{-2}
$m_h = 125.7(4)$ GeV
$m_Z = 91.1876(21)$ GeV
$m_W = 80.385(15)$ GeV
$\Gamma_Z = 2.4952(23)$ GeV

In the SM, as we can see from Fig. 2, the function $d^2\Gamma/da_1da_2$ has peaks at $\sqrt{a_1} = m_Z$ and $\sqrt{a_2} = m_Z$, resulting from the quantities $D(a_1)$ and $D(a_2)$ in (8).

We calculate the ratio of a typical value of $d^2\Gamma/da_1da_2$ in the SM on the peaks to its typical value in an area where $\sqrt{a_1}$ and $\sqrt{a_2}$ significantly differ from m_Z (we call this area the "plateau"). As indicative values of $\sqrt{a_1}$ and $\sqrt{a_2}$ on the peaks, we take $\sqrt{a_1} = m_Z$, $\sqrt{a_2} = (m_h - m_Z)/2$ and $\sqrt{a_1} = (m_h - m_Z)/2$, $\sqrt{a_2} = m_Z$ (see (2)), and values on the "plateau" are chosen as $\sqrt{a_1} = \sqrt{a_2} = m_Z/2$. It follows from (8) that in the SM for any f_1 and f_2, the values of $d^2\Gamma/da_1da_2$ at $\sqrt{a_1} = m_Z$ or $\sqrt{a_2} = m_Z$ are approximately 100 times as great as values of this function on the "plateau".

If $m_X \neq m_h$ but is just greater than m_Z, then $\sqrt{a_1}$ and/or $\sqrt{a_2}$ can be equal to m_Z (according to (2)), and, consequently, the behavior of the function $d^2\Gamma/da_1da_2$ in the SM is then similar to that in the case $m_X = m_h$. That is why for any $m_X > m_Z$ and for any final fermions, the differential width $d^2\Gamma/da_1da_2$ in the SM has a sharp maximum at $\sqrt{a_1} = m_Z$ or $\sqrt{a_2} = m_Z$. Therefore, if $|a_Z| \approx 1$, $b_Z \approx 0$, and $c_Z \approx 0$ (which is the

case of a small distinction between the couplings and their SM values), $d^2\Gamma/da_1da_2$ also has a sharp maximum at $\sqrt{a_1} = m_Z$ or $\sqrt{a_2} = m_Z$ if $m_X > m_Z$.

2.3. Applicability limits of the narrow-Z-width approximation

In Refs. [27–29], the accuracy of the narrow-width approximation has been studied for the calculation of the total widths of various decays along with the total and differential cross sections of various processes. It is shown that in many cases (especially for processes beyond the SM), this approximation is not applicable. In this connection, the question arises whether the narrow-Z-width approximation is applicable to obtaining the differential width $d\Gamma/da_2$ by means of integrating $d^2\Gamma/da_1da_2$. In this section, we find the interval of all the a_2 values for which the approximate integration is valid.

We consider the m_X values such that $m_X > m_Z$ and the dependences of $a_Z(a_1, a_2)$, $b_Z(a_1, a_2)$, and $c_Z(a_1, a_2)$ such that for any f_1 and f_2, $d^2\Gamma/da_1da_2$ has a sharp maximum when $\sqrt{a_1} = m_Z$ or $\sqrt{a_2} = m_Z$ (an example of such dependences is $|a_Z| \approx 1$, $b_Z \approx 0$, $c_Z \approx 0$). Calculating the differential width $d\Gamma/da_2$, we can then use the narrow-Z-width approximation:

$$\frac{d\Gamma}{da_2} = \int\limits_0^{(m_X-\sqrt{a_2})^2} da_1 \frac{d^2\Gamma}{da_1da_2} \approx$$

$$\approx \int\limits_0^{(m_X-\sqrt{a_2})^2} da_1 \frac{\pi}{m_Z\Gamma_Z}\delta(a_1 - m_Z^2) f(a_1, a_2) =$$

$$= \frac{\pi}{m_Z\Gamma_Z} f(m_Z^2, a_2) \quad \forall\sqrt{a_2} \in (0, m_X - m_Z - \Delta], \quad (9)$$

where Δ is some positive quantity and

$$f(a_1, a_2) \equiv \frac{\sqrt{2}G_F^3 m_Z^8}{9(2\pi)^5 m_X^3}(a_{f_1}^2 + v_{f_1}^2)(a_{f_2}^2 + v_{f_2}^2)\times$$

$$\times \frac{\lambda^{1/2}(m_X^2, a_1, a_2)a_1a_2}{D(a_2)} \sum_{p=0,\parallel,\perp} |A_p|^2. \quad (10)$$

We have $\Delta > 0$ since we can use the approximation

$$\frac{d^2\Gamma}{da_1da_2} = \frac{\pi}{m_Z\Gamma_Z}\delta(a_1 - m_Z^2) f(a_1, a_2)$$

in Eq. (9) only when $\sqrt{a_2} < m_X - m_Z$, because if $\sqrt{a_2}$ approaches $m_X - m_Z$, the peak of $d^2\Gamma/da_1da_2$ at $\sqrt{a_1} = m_Z$ becomes less sharp and disappears at $\sqrt{a_2} = m_X - m_Z$ (see Fig. 2 and Eq. (8)). However, the derivation of (9) does not allow estimating the accuracy of the formula

$$\frac{d\Gamma}{da_2} \approx \frac{\pi}{m_Z\Gamma_Z} f(m_Z^2, a_2)$$

at a given value of $\sqrt{a_2}$, and therefore it is not clear what value of Δ should be chosen.

To clarify this point, let us derive the formula for $d\Gamma/da_2$ as

$$\frac{d\Gamma}{da_2} = \int\limits_0^{(m_X-\sqrt{a_2})^2} da_1 \frac{d^2\Gamma}{da_1da_2} \approx \int\limits_{m_Z^2-\varepsilon_1}^{m_Z^2+\varepsilon_2} da_1 \frac{d^2\Gamma}{da_1da_2} =$$

$$= \int\limits_{m_Z^2-\varepsilon_1}^{m_Z^2+\varepsilon_2} da_1 \frac{f(a_1, a_2)}{(a_1 - m_Z^2)^2 + (m_Z\Gamma_Z)^2} \approx$$

$$\approx \int\limits_{m_Z^2-\varepsilon_1}^{m_Z^2+\varepsilon_2} da_1 \frac{f(m_Z^2, a_2)}{(a_1 - m_Z^2)^2 + (m_Z\Gamma_Z)^2} =$$

$$= \frac{\arctan\dfrac{\varepsilon_2}{m_Z\Gamma_Z} + \arctan\dfrac{\varepsilon_1}{m_Z\Gamma_Z}}{m_Z\Gamma_Z} f(m_Z^2, a_2) \approx$$

$$\approx \frac{\pi}{m_Z\Gamma_Z} f(m_Z^2, a_2), \quad (11)$$

where ε_1 and ε_2 are some positive quantities such that $m_Z\Gamma_Z \ll \varepsilon_j \ll m_Z^2$, and a_2 takes values in the interval $\left(0, \left(m_X - \sqrt{m_Z^2 + \varepsilon_2}\right)^2\right]$.

One of the approximations used in Eq. (11) is the switch from the integration over the interval $\left(0, \left(m_X - \sqrt{a_2}\right)^2\right)$ to the integration over the interval $(m_Z^2 - \varepsilon_1, m_Z^2 + \varepsilon_2)$. Hence, $m_Z^2 - \varepsilon_1$ has to be greater than or equal to $4m_{f_1}^2$ (which is the case because $\varepsilon_1 \ll \ll m_Z^2$) and $m_Z^2 + \varepsilon_2$ has to be less than or equal to $\left(m_X - \sqrt{a_2}\right)^2$, i. e., $a_2 \le \left(m_X - \sqrt{m_Z^2 + \varepsilon_2}\right)^2$. The latter inequality restricts the interval of the a_2 values for which these approximations are applicable. Consequently, in order to apply them for an interval of a_2 values as long as possible, we should use the minimum ε_2 value at which the approximations are valid.

In obtaining (11), we also used the approximation $A \approx \pi$, where

$$A \equiv \arctan\frac{\varepsilon_2}{m_Z\Gamma_Z} + \arctan\frac{\varepsilon_1}{m_Z\Gamma_Z}.$$

We define ε_1 as $\varepsilon_1 \equiv m_Z\sqrt{m_Z\Gamma_Z}$, which follows from

$$\frac{\varepsilon_1}{m_Z\Gamma_Z} = \frac{m_Z^2}{\varepsilon_1}.$$

For the considered ε_2 values, the values of A and $m_h - \sqrt{m_Z^2 + \varepsilon_2}$ listed in Table 2 specify the accuracy of

Table 2. Values of A ($\varepsilon_1 \equiv m_Z\sqrt{m_Z\Gamma_Z}$) and of $m_h - \sqrt{m_Z^2+\varepsilon_2}$ at various values of ε_2

ε_2	A	$m_h - \sqrt{m_Z^2+\varepsilon_2}$, GeV
0	0.45π	34.51
$m_Z\Gamma_Z$	0.70π	33.27
$2m_Z\Gamma_Z$	0.80π	32.05
$3m_Z\Gamma_Z$	0.85π	30.84
$4m_Z\Gamma_Z$	0.87π	29.65

the approximation $A \approx \pi$ and the maximum value of $\sqrt{a_2}$ at which the narrow-Z-width approximation is applicable in the case $X = h$.

According to Table 2, if $\varepsilon_2 < 3m_Z\Gamma_Z$, then $A < 0.85\pi$ and, in view of the big difference between A and π, we do not apply approximations (11) for such values of ε_2. Hence, we use $\varepsilon_2 = 3m_Z\Gamma_Z$. It follows from (11) that

$$\frac{d\Gamma}{da_2} \approx \frac{\sqrt{2}G_F^3 m_Z^9}{9\cdot 2^5\pi^4 m_X^3\Gamma_Z}(a_{f_1}^2+v_{f_1}^2)(a_{f_2}^2+v_{f_2}^2)\times \times\frac{\lambda^{1/2}(m_X^2,m_Z^2,a_2)a_2}{D(a_2)}\times \times\sum_{p=0,\parallel,\perp}|A'_p|^2\ \forall\ \sqrt{a_2}\in\left(0, m_X-\sqrt{m_Z^2+\varepsilon_2}\right], \quad (12)$$

where $A'_p \equiv A_p(m_Z^2, a_2)$ $(p = 0, \parallel, \perp)$.

We note that when plotting dependences of $(1/\Gamma)(d\Gamma/da_2)$ on $\sqrt{a_2}$ in Refs. [14, 16, 17], formulas for $d\Gamma/da_2$ that correspond to (12) have been used, but these graphs were plotted for $\sqrt{a_2} \le m_X - m_Z$, although Eq. (11) is not valid at $\varepsilon_2 = 0$ (see Table 2), and therefore, the plotted dependences significantly differ from the true ones in the interval

$$\sqrt{a_2}\in\left(m_X-\sqrt{m_Z^2+3m_Z\Gamma_Z}, m_X-m_Z\right].$$

2.4. An inequality constraining a'_{hZ}, b'_{hZ}, and c'_{hZ} from the CMS data

According to [3],

$$\frac{\sigma(pp\to h)\dfrac{\Gamma(h\to Z_1^*Z_2^*\to 4l)}{\Gamma_h}}{\sigma_{SM}(pp\to h)\dfrac{\Gamma_{SM}(h\to Z_1^*Z_2^*\to 4l)}{\Gamma_{h\,SM}}} = 0.93^{+0.26}_{-0.23}(\text{stat})^{+0.13}_{-0.09}(\text{syst}), \quad (13)$$

where $\sigma(pp \to h)$ is the cross section for production of h in pp collisions,

Table 3. Experimental and theoretical results for the total production cross section of the Higgs boson in pp collisions and for its total width

$\sigma(pp\to h) = 33.0\pm 5.3(\text{stat})\pm 1.6(\text{syst})$ pb at $\sqrt{s} = 8$ TeV [31]
$\sigma_{SM}(pp\to h) = 22.09$ pb (uncertainties not available) at $\sqrt{s} = 8$ TeV [32]
$\Gamma_h < 22$ MeV at 95% confidence level (CL) [33]
$\Gamma_{h\,SM} = 4.15\pm 0.16$ MeV [34]

$$\Gamma(h\to Z_1^*Z_2^*\to 4l)\equiv\Gamma(h\to Z_1^*Z_2^*\to 4e)+ +\Gamma(h\to Z_1^*Z_2^*\to 4\mu)+\Gamma(h\to Z_1^*Z_2^*\to 2e2\mu)= =2\Gamma(h\to Z_1^*Z_2^*\to 4e)+\Gamma(h\to Z_1^*Z_2^*\to 2e2\mu), \quad (14)$$

Γ_h is the total width of the boson h, and $\sigma_{SM}(pp\to h)$, $\Gamma_{SM}(h\to Z_1^*Z_2^*\to 4l)$, and $\Gamma_{h\,SM}$ are the respective SM predictions for $\sigma(pp\to h)$, $\Gamma(h\to Z_1^*Z_2^*\to 4l)$, and Γ_h at $m_h = 125.6$ GeV. In obtaining (13), the CMS collaboration has combined data from pp collisions corresponding to an integrated luminosity of 5.1 fb^{-1} at the center-of-mass energy $\sqrt{s} = 7$ TeV and 19.7 fb^{-1} at $\sqrt{s} = 8$ TeV.

We consider the case where the functions $|a'_{hZ}|$, $|b'_{hZ}|$, $|c'_{hZ}|$, and $\cos(\arg b'_{hZ} - \arg a'_{hZ})$ do not depend on a_2. We set

$$a'_{hZ}\equiv a_{hZ}(m_Z^2,a_2),\quad b'_{hZ}\equiv b_{hZ}(m_Z^2,a_2),$$
$$c'_{hZ}\equiv c_{hZ}(m_Z^2,a_2).$$

Then using the approximation

$$\frac{\sigma(pp\to h)}{\Gamma_h}\approx\frac{\sigma_{SM}(pp\to h)}{\Gamma_{h\,SM}} \quad (15)$$

and Eqs. (13) (within one standard deviation), (A.10), and (A.13) (see Appendix), we derive the relation

$$|a'_{hZ}|^2+0.015\,|b'_{hZ}|^2+0.177\,\mathrm{Re}(a'^*_{hZ}b'_{hZ})+ +0.037\,|c'_{hZ}|^2\in[0.68,\,1.22]. \quad (16)$$

In obtaining (16), we substituted the central values of m_h, m_Z, Γ_Z listed in Table 1 in Eq. (A.10). We note that the latter equation is derived at the tree level and without allowance for the interference term connected with the permutation of the identical fermions in the case where $f_1 = f_2$. The interference contribution to $\Gamma(h\to Z_1^*Z_2^*\to 4l)$ at the tree level is expected to be negligible since in the SM at $m_h = 140$ GeV it amounts to 2.99 % (see Table 1 in Ref. [30]). Using the data in

Table 3 and considering two-sigma errors where available, we obtain that

$$\frac{\sigma(pp\to h)/\Gamma_h}{\sigma_{SM}(pp\to h)/\Gamma_{h\,SM}}\in(0.17,\infty) \tag{17}$$

at $\sqrt{s}=8$ TeV, which means that approximation (15) does not contradict the experimental limits.

Moreover, assuming that all the couplings of the Higgs boson except a_{hZ}, b_{hZ}, and c_{hZ} are equal to their SM values, we can verify (15). In this case, the only anomalous contribution to Γ_h comes from $\Gamma(h\to Z_1^*Z_2^*)$, which in the SM amounts to only about 2.81 % [34] of the total Higgs boson width, and therefore Γ_h is unlikely to substantially differ from its SM prediction. Besides, inequality (16) means that

$$\frac{|\Gamma(h\to Z_1^*Z_2^*)-\Gamma_{SM}(h\to Z_1^*Z_2^*)|}{\Gamma_{SM}(h\to Z_1^*Z_2^*)}\in[0,0.32]$$

because its left-hand side is

$$\frac{\Gamma(h\to Z_1^*Z_2^*\to 4l)}{\Gamma_{SM}(h\to Z_1^*Z_2^*\to 4l)}=\frac{\Gamma(h\to Z_1^*Z_2^*)}{\Gamma_{SM}(h\to Z_1^*Z_2^*)}$$

(see (13) and (A.10)). For this reason, Eq. (16) implies that the relative change of Γ_h is less than $2.81\,\%\times$ $\times\,0.32\approx 0.90\%$, and, consequently, (16) is consistent with the approximation $\Gamma_h\approx\Gamma_{h\,SM}$.

The leading contribution to the Higgs boson production cross section $\sigma_{SM}(pp\to h)$ comes from the gluon fusion process $gg\to h$, which is independent of the hZZ vertex. The processes involving the hZZ interaction, i. e., the Higgs-strahlung Zh and the Z boson fusion, constitute much less parts of $\sigma_{SM}(pp\to h)$. Specifically, at $\sqrt{s}=8$ TeV, they can be estimated as 0.41 pb and 0.70 pb respectively [32]. The total production cross section at this energy is 22.09 pb (see Table 3), and hence the processes of interest contribute about 5% of the total cross section. That is why it seems improbable that the couplings a_{hZ}, b_{hZ}, and c_{hZ} provide a significant difference between $\sigma(pp\to h)$ and $\sigma_{SM}(pp\to h)$. However, a derivation of the dependence of the total production cross section on the hZZ couplings would require a separate study.

Summarizing the discussion of approximation (15), we can infer that, first, it is consistent with the available data [31, 33] and, second, under the assumption that the only anomalous Higgs boson couplings are related to the hZZ vertex, Eq. (15) is most likely to be valid due to the small contributions of the hZZ vertex to Γ_h and $\sigma(pp\to h)$.

2.5. Constraints on a'_{hZ}, b'_{hZ}, and c'_{hZ}

Inequality (16) constrains the whole six-dimensional space formed by the real and imaginary parts of the couplings a'_{hZ}, b'_{hZ}, and c'_{hZ} to the set of ellipsoids allowed by (13). We note that a similar interpretation has been suggested in Ref. [35].

It follows from (16) that the variant $a'_{hZ}=0$, $b'_{hZ}=$ $=0$, $c'_{hZ}=1$ (negative CP parity of the boson h) is excluded. We now find constraints on the values of b'_{hZ} and c'_{hZ}, assuming that a'_{hZ} is taken from the SM, i. e., $|a'_{hZ}|=1$ or $a'_{hZ}=1$. Then

$$|a'_{hZ}|=1 \quad\text{and}\quad b'_{hZ}=0\Rightarrow|c'_{hZ}|\in[0,\,2.44], \tag{18a}$$

$$a'_{hZ}=1 \quad\text{and}\quad c'_{hZ}=0 \quad\text{and}\quad \operatorname{Im}b'_{hZ}=$$
$$=0\Rightarrow b'_{hZ}\in([-12.66,-9.31]\cup[-2.22,1.14]), \tag{18b}$$

$$a'_{hZ}=1 \quad\text{and}\quad c'_{hZ}=0 \quad\text{and}\quad \operatorname{Re}b'_{hZ}=$$
$$=0\Rightarrow \operatorname{Im}b'_{hZ}\in[-3.84,\,3.84]. \tag{18c}$$

We compare (18) with the hZZ coupling constraints obtained by the CMS [36] and ATLAS [37] collaborations. For this purpose, we first express our XZZ couplings in terms of the CMS ones $\tilde a_1$, $\tilde a_2$, $\tilde a_3$ (we let a_1, a_2, a_3 from [36] be denoted as $\tilde a_1$, $\tilde a_2$, $\tilde a_3$ to avoid confusion):

$$a_Z=\tilde\alpha\left(\tilde a_1-\exp(i\phi_{\Lambda_1})\frac{a_1+a_2}{\Lambda_1^2}+\right.$$
$$\left.+\,\frac{m_X^2-a_1-a_2}{m_Z^2}\tilde a_2\right), \tag{19a}$$

$$b_Z=-2\tilde\alpha\frac{m_X^2}{m_Z^2}\tilde a_2, \tag{19b}$$

$$c_Z=-i\tilde\alpha\frac{m_X^2}{m_Z^2}\tilde a_3, \tag{19c}$$

where $\tilde\alpha\equiv\alpha_0 v/2$, α_0 is the proportionality factor of the amplitude $A(HZZ)$ of the transition $X\to Z_1^*Z_2^*$ (see Eq. (1) in [36], $v\equiv 1/\sqrt{\sqrt{2}G_F}$ is the vacuum expectation value of the Higgs field, Λ_1 is a scale of physics beyond the SM, and ϕ_{Λ_1} is the phase in the term with Λ_1. In general, $\tilde a_1$, $\tilde a_2$, and $\tilde a_3$ may depend on a_1 and a_2, but in [36] they are set to be constant. The ATLAS XZZ couplings α, κ_{SM}, κ_{HZZ}, and κ_{AZZ} are related to the CMS ones as

$$\tilde\alpha\left(\tilde a_1-\exp(i\phi_{\Lambda_1})\frac{a_1+a_2}{\Lambda_1^2}\right)=\kappa_{SM}\cos\alpha,$$
$$\tilde\alpha\tilde a_2=\frac{v}{4\Lambda}\kappa_{HZZ}\cos\alpha, \tag{20}$$
$$\tilde\alpha\tilde a_3=\frac{v}{4\Lambda}\kappa_{AZZ}\sin\alpha,$$

where Λ is the EFT energy scale. We note that comparing the Lagrangian (1) in [36] with the one describing the interaction of the SM Higgs field with ZZ and

Table 4. The CMS [36] and ATLAS [37] 95 % CL allowed regions for hZZ couplings. The last row shows the conditions under which these regions were derived

CMS		ATLAS	
$\dfrac{\tilde{a}_2}{\tilde{a}_1}$	$\dfrac{\tilde{a}_3}{\tilde{a}_1}$	$\dfrac{\tilde{\kappa}_{HZZ}}{\kappa_{SM}}$	$\dfrac{\tilde{\kappa}_{AZZ}}{\kappa_{SM}}\tan\alpha$
$[-2.28,-1.88]\cup[-0.69,\infty)$	$[-2.05, 2.19]$	$(-0.75, 2.45)$	$(-2.85, 0.95)$
$\operatorname{Im}\dfrac{\tilde{a}_2}{\tilde{a}_1}=0$, $\phi_{\Lambda_1}=0$ or π	$\operatorname{Im}\dfrac{\tilde{a}_3}{\tilde{a}_1}=0$, $\phi_{\Lambda_1}=0$ or π	$\kappa_{AZZ}=0$	$\kappa_{HZZ}=0$

Table 5. Our allowed regions for the ATLAS hZZ couplings. The last two rows show the conditions under which these regions were derived

$\dfrac{\tilde{\kappa}_{HZZ}}{\kappa_{SM}}$	$\dfrac{\tilde{\kappa}_{AZZ}}{\kappa_{SM}}\tan\alpha$	$\dfrac{\operatorname{Im}\tilde{\kappa}_{HZZ}}{\operatorname{Re}\kappa_{SM}}$
$[-2.38,-1.89]\cup[-0.24, 1.13]$	$[-1.28, 1.28]$	$[-1.01, 1.01]$
$a_2=(m_h-m_Z)^2/2$ in (19a),	$\lvert a'_{hZ}\rvert=1$, $\kappa_{HZZ}=0$, $\operatorname{Im}\dfrac{\tilde{\kappa}_{AZZ}}{\kappa_{SM}}=0$	$a_2=(m_h-m_Z)^2/2$ in (19a),
$a'_{hZ}=1$, $\kappa_{AZZ}\sin\alpha=0$, $\operatorname{Im}\kappa_{HZZ}=0$		$a'_{hZ}=1$, $\kappa_{AZZ}\sin\alpha=0$, $\operatorname{Re}\kappa_{HZZ}=0$

W^-W^+, we can deduce that the coupling g_{HZZ} from (1) in [36] is equal to $2m_Z^2/v$. In [36], the couplings α, κ_{SM}, κ_{HZZ}, and κ_{AZZ} are considered constant and real.

In Refs. [36, 37], 95 % CL allowed regions for hZZ couplings are reported (see Table 4). We note that

$$\tilde{\kappa}_{HZZ}\equiv\frac{v}{4\Lambda}\kappa_{HZZ},\quad \tilde{\kappa}_{AZZ}\equiv\frac{v}{4\Lambda}\kappa_{AZZ}, \tag{21}$$

$$\begin{aligned}\frac{\tilde{\kappa}_{HZZ}}{\kappa_{SM}}&=-\frac{m_Z^2\,b_Z}{2m_X^2\,a_Z+(m_X^2-a_1-a_2)\,b_Z},\\ \frac{\tilde{\kappa}_{AZZ}}{\kappa_{SM}}\tan\alpha&=\frac{2im_Z^2\,c_Z}{2m_X^2\,a_Z+(m_X^2-a_1-a_2)\,b_Z}\end{aligned} \tag{22}$$

and in the limit $\Lambda_1\to\infty$, the CMS and ATLAS ratios coincide:

$$\begin{aligned}\frac{\tilde{a}_2}{\tilde{a}_1}&=\lim_{\Lambda_1\to\infty}\frac{\tilde{\kappa}_{HZZ}}{\kappa_{SM}},\\ \frac{\tilde{a}_3}{\tilde{a}_1}&=\lim_{\Lambda_1\to\infty}\left(\frac{\tilde{\kappa}_{AZZ}}{\kappa_{SM}}\tan\alpha\right).\end{aligned} \tag{23}$$

Following [37], we assume the ATLAS hZZ couplings to be constant. Then considering the case $\kappa_{HZZ}=0$, we find that our couplings a_{hZ}, b_{hZ}, and c_{hZ} are also constant (see (19) and (20)), and using (18a) we obtain the allowed interval for $\tilde{\kappa}_{AZZ}\tan\alpha/\kappa_{SM}$ (see Table 5). However, in the case $\kappa_{HZZ}=0$, results (18b) and (18c) only show that h may be the SM Higgs boson, and they do not therefore constrain any hZZ couplings.

If $\kappa_{HZZ}\neq 0$, then a_{hZ} acquires a dependence on the invariant masses squared a_1 and a_2, and therefore constraints (16) and (18) become invalid because they were derived under the assumption that $|a'_{hZ}|$ is independent of a_2. Therefore, to constrain the ATLAS couplings in the case $\kappa_{HZZ}\neq 0$, we start with Eqs. (13) and (15), which demonstrate that within one standard deviation,

$$\frac{\Gamma(h\to Z_1^*Z_2^*\to 4l)}{\Gamma_{SM}(h\to Z_1^*Z_2^*\to 4l)}\in[0.68,\,1.22].$$

To obtain Γ, we have to calculate integral (A.1) for a'_Z depending on a_2. Taking the integration limits into account, we replace a_2 with $(m_X-m_Z)^2/2$ in the expression for a'_Z (see (19a) and (20)) and thus derive Eq. (A.10) where a_Z has expression (19a) with $a_2=$ $=(m_X-m_Z)^2/2$. This means that if κ_{HZZ} is not zero, we can use (16) and (18b), (18c) with a'_{hZ} determined by Eq. (19a) where a_2 is replaced by $(m_h-m_Z)^2/2$. This conclusion allows us to constrain $\tilde{\kappa}_{HZZ}/\kappa_{SM}$ and $\operatorname{Im}\tilde{\kappa}_{HZZ}/\operatorname{Re}\kappa_{SM}$, as we can see in Table 5.

We note that results (16) and (18), along with the regions shown in Table 5, are estimated with consideration of the one-sigma interval in (13), approximation (15), the central values of m_h, m_Z, and Γ_Z from Table 1, and Eq. (A.10). Comparing Tables 4 and 5, we note significant overlaps between the constraints reported in [36, 37] and ours. In addition, we present the

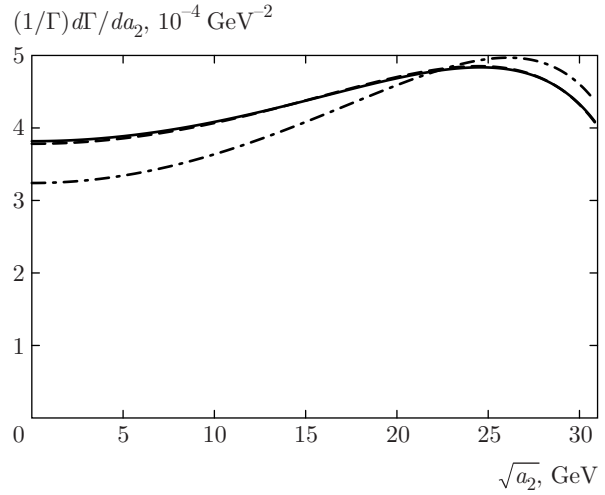

Fig. 3. The distribution $(1/\Gamma)d\Gamma/da_2$ as a function of $\sqrt{a_2}$ for the decay $h \to Z_1^* Z_2^* \to f_1\bar{f}_1 f_2 \bar{f}_2$ in the case $|a'_{hZ}| = 1$, $b'_{hZ} = 0$, $c'_{hZ} = 0$ (solid line); $|a'_{hZ}| = 1$, $b'_{hZ} = 0$, $|c'_{hZ}| = 0.5$ (dashed line); $a'_{hZ} = 1$, $b'_{hZ} = -0.5$, $c'_{hZ} = 0$ (dash-dotted line)

allowed interval for the ratio $\operatorname{Im}\tilde{\kappa}_{HZZ}/\operatorname{Re}\kappa_{SM}$ unconstrained in Refs. [36, 37].

We choose the following sets of values of a'_{hZ}, b'_{hZ}, and c'_{hZ}:

$$\begin{aligned} &|a'_{hZ}| = 1, \quad b'_{hZ} = 0, \quad c'_{hZ} = 0, \\ &a'_{hZ} = 1, \quad b'_{hZ} = 0, \quad c'_{hZ} = 0.5, \\ &a'_{hZ} = 1, \quad b'_{hZ} = 0, \quad c'_{hZ} = 0.5i, \\ &a'_{hZ} = 1, \quad b'_{hZ} = -0.5, \quad c'_{hZ} = 0, \end{aligned} \tag{24}$$

and

$$a'_{hZ} = 1, \quad b'_{hZ} = -0.5i, \quad c'_{hZ} = 0, \tag{25}$$

which are consistent with constraints (18). The sets (24) and (25) are to be used for examining further results.

Regarding the values chosen in (24) and (25), we note that even in the SM, the couplings b_{hZ} and c_{hZ} acquire small values due to electroweak radiative corrections, with $\operatorname{Im} b_{hZ}$ and $\operatorname{Im} c_{hZ}$ coming from the absorptive parts of the corresponding loop diagrams. We assume in Eqs. (24) and (25) that the hZZ vertex may be significantly modified by physics beyond the SM.

It is of interest to study the distribution $(1/\Gamma) \times (d\Gamma/da_2)$ as a function of $\sqrt{a_2}$ for various sets of a'_Z, b'_Z, and c'_Z. Here, $a'_Z \equiv a_Z(m_Z^2, a_2)$, $b'_Z \equiv b_Z(m_Z^2, a_2)$, and $c'_Z \equiv c_Z(m_Z^2, a_2)$. In accordance with (8), the function $(1/\Gamma)(d\Gamma/da_2)$ is independent of the final fermion state. Figure 3 shows this observable in the case $X = h$.

As we can see from Fig. 3, the function $(1/\Gamma) \times (d\Gamma/da_2)$ is sensitive to b'_{hZ} and almost insensitive to c'_{hZ}. For this reason, measuring this distribution with sufficient accuracy can lead to significant constraints on the values of b'_{hZ}. However, we should keep in mind that this conclusion is obtained in the case where $|a'_{hZ}|$, $|b'_{hZ}|$, $|c'_{hZ}|$, and $\cos(\arg b'_{hZ} - \arg a'_{hZ})$ are independent of a_2, and their a_2-dependence can considerably modify the dependence of $(1/\Gamma)(d\Gamma/da_2)$. In Sec. 2.6, we develop methods for obtaining constraints on the dependences of a'_Z, b'_Z, and c'_Z on a_2.

2.6. Connection between the helicity coefficients of the decay $X \to Z_1^* Z_2^*$ and observables

We now consider arbitrary dependences of $a_Z(a_1, a_2)$, $b_Z(a_1, a_2)$, and $c_Z(a_1, a_2)$ such that the differential width

$$\frac{d^5\Gamma}{da_1 da_2 d\theta_1 d\theta_2 d\varphi}$$

has a sharp maximum as a function of a_1 and a_2 at $\sqrt{a_1} = m_Z$ or $\sqrt{a_2} = m_Z$ for any f_1 and f_2. From Eq. (5), using approximations analogous to those used in deriving the formulas (11) and (A.1), we integrate over a_1 and some of the angular variables. Then under the condition $\sqrt{a_2} \in \left(0, m_X - \sqrt{m_Z^2 + \varepsilon_2}\right]$, we obtain the following relations between observables $O_i(a_2)$ and the helicity coefficients:

$$\begin{aligned} O_1^{(1)}(a_2) &\equiv \left(\frac{d\Gamma}{da_2}\right)^{-1} \left(\int\limits_0^{\pi/2} d\theta_1 \frac{d^2\Gamma}{da_2 d\theta_1} - \right. \\ &\left. - \int\limits_{\pi/2}^{\pi} d\theta_1 \frac{d^2\Gamma}{da_2 d\theta_1} \right) = -\frac{3}{2} A_{f_1} \frac{\operatorname{Re}(A'^*_{\parallel} A'_{\perp})}{\sum_p |A'_p|^2}, \\ O_1^{(2)}(a_2) &\equiv \left(\frac{d\Gamma}{da_2}\right)^{-1} \left(\int\limits_0^{\pi/2} d\theta_2 \frac{d^2\Gamma}{da_2 d\theta_2} - \right. \\ &\left. - \int\limits_{\pi/2}^{\pi} d\theta_2 \frac{d^2\Gamma}{da_2 d\theta_2} \right) = -\frac{3}{2} A_{f_2} \frac{\operatorname{Re}(A'^*_{\parallel} A'_{\perp})}{\sum_p |A'_p|^2}. \end{aligned} \tag{26}$$

We can write these two formulas as

$$O_1^{(1,2)}(a_2) \equiv \left(\frac{d\Gamma}{da_2}\right)^{-1}\left(\int\limits_0^{\pi/2} d\theta_{1,2}\frac{d^2\Gamma}{da_2 d\theta_{1,2}} - \right.$$
$$\left. - \int\limits_{\pi/2}^{\pi} d\theta_{1,2}\frac{d^2\Gamma}{da_2 d\theta_{1,2}}\right) = -\frac{3}{2}A_{f_{1,2}}\frac{\mathrm{Re}(A'^{*}_{\parallel}A'_{\perp})}{\sum_p |A'_p|^2}. \quad (27)$$

Then we deduce that

$$O_2(a_2) \equiv \left(\frac{d\Gamma}{da_2}\right)^{-1}\left(\int\limits_{\pi/2-\beta}^{\pi/2-\alpha} d\theta_2\frac{d^2\Gamma}{da_2 d\theta_2} + \right.$$
$$\left. + \int\limits_{\pi/2+\alpha}^{\pi/2+\beta} d\theta_2 \ldots\right) = \left(\frac{d\Gamma}{da_2}\right)^{-1} \times$$
$$\times \left(\int\limits_{\pi/2-\beta}^{\pi/2-\alpha} d\theta_1\frac{d^2\Gamma}{da_2 d\theta_1} + \int\limits_{\pi/2+\alpha}^{\pi/2+\beta} d\theta_1 \ldots\right) = \quad (28)$$
$$= \frac{1}{4}\Big((\sin\beta - \sin\alpha)(3 + \sin^2\alpha + \sin^2\beta +$$
$$+ \sin\alpha\sin\beta) + 3\frac{|A'_0|^2}{\sum_p |A'_p|^2} \times$$
$$\times (\sin\beta\cos^2\beta - \sin\alpha\cos^2\alpha)\Big),$$
$$0 \le \alpha < \beta \le \frac{\pi}{2},$$

$$O_3(a_2) \equiv \left(\frac{d\Gamma}{da_2}\right)^{-1}\left(\int\limits_0^{\pi/2} d\theta_2\left(\int\limits_0^{\pi/2} d\theta_1\frac{d^3\Gamma}{da_2 d\theta_1 d\theta_2} - \right.\right.$$
$$\left.\left. - \int\limits_{\pi/2}^{\pi} d\theta_1\frac{d^3\Gamma}{da_2 d\theta_1 d\theta_2}\right) - \int\limits_{\pi/2}^{\pi} d\theta_2 \ldots\right) =$$
$$= \frac{9}{16}A_{f_1}A_{f_2}\frac{|A'_{\parallel}|^2 + |A'_{\perp}|^2}{\sum_p |A'_p|^2}, \quad (29)$$

$$O_4(a_2) \equiv \left(\frac{d\Gamma}{da_2}\right)^{-1}\left(\int\limits_0^{\pi/4} d\varphi\frac{d^2\Gamma}{da_2 d\varphi} - \int\limits_{\pi/4}^{3\pi/4} d\varphi \ldots + \right.$$
$$+ \int\limits_{3\pi/4}^{5\pi/4} d\varphi \ldots - \int\limits_{5\pi/4}^{7\pi/4} d\varphi \ldots + \left.\int\limits_{7\pi/4}^{2\pi} d\varphi \ldots\right) =$$
$$= \frac{1}{2\pi}\frac{|A'_{\parallel}|^2 - |A'_{\perp}|^2}{\sum_p |A'_p|^2}, \quad (30)$$

$$O_5(a_2) \equiv \left(\frac{d\Gamma}{da_2}\right)^{-1}\left(\int\limits_0^{\pi/2} d\varphi\frac{d^2\Gamma}{da_2 d\varphi} - \int\limits_{\pi/2}^{\pi} d\varphi \ldots + \right.$$
$$\left. + \int\limits_{\pi}^{3\pi/2} d\varphi \ldots - \int\limits_{3\pi/2}^{2\pi} d\varphi \ldots\right) =$$
$$= -\frac{1}{\pi}\frac{\mathrm{Im}(A'^{*}_{\parallel}A'_{\perp})}{\sum_p |A'_p|^2}, \quad (31)$$

$$O_6(a_2) \equiv \left(\frac{d\Gamma}{da_2}\right)^{-1}\left(\int\limits_0^{\pi/2} d\varphi\frac{d^2\Gamma}{da_2 d\varphi} - \int\limits_{\pi/2}^{3\pi/2} d\varphi \ldots + \right.$$
$$\left. + \int\limits_{3\pi/2}^{2\pi} d\varphi \ldots\right) = \frac{9}{32}\sqrt{2}\pi A_{f_1}A_{f_2}\frac{\mathrm{Re}(A'^{*}_{0}A'_{\parallel})}{\sum_p |A'_p|^2}, \quad (32)$$

$$O_7^{(1,2)}(a_2) \equiv \left(\frac{d\Gamma}{da_2}\right)^{-1} \times$$
$$\times \left(\int\limits_0^{\pi} d\varphi\left(\int\limits_0^{\pi/2} d\theta_{1,2}\frac{d^3\Gamma}{da_2 d\theta_{1,2} d\varphi} - \right.\right.$$
$$\left.\left. - \int\limits_{\pi/2}^{\pi} d\theta_{1,2}\frac{d^3\Gamma}{da_2 d\theta_{1,2} d\varphi}\right) - \int\limits_{\pi}^{2\pi} d\varphi \ldots\right) =$$
$$= \frac{3}{8}\sqrt{2}A_{f_{2,1}}\frac{\mathrm{Im}(A'^{*}_{0}A'_{\parallel})}{\sum_p |A'_p|^2}, \quad (33)$$

$$O_8^{(1,2)}(a_2) \equiv \left(\frac{d\Gamma}{da_2}\right)^{-1} \times$$
$$\times \left(\int\limits_0^{\pi/2} d\varphi\left(\int\limits_0^{\pi/2} d\theta_{1,2}\frac{d^3\Gamma}{da_2 d\theta_{1,2} d\varphi} - \right.\right.$$
$$\left.\left. - \int\limits_{\pi/2}^{\pi} d\theta_{1,2}\frac{d^3\Gamma}{da_2 d\theta_{1,2} d\varphi}\right) - \int\limits_{\pi/2}^{3\pi/2} d\varphi \ldots + \int\limits_{3\pi/2}^{2\pi} d\varphi \ldots\right) =$$
$$= -\frac{3}{8}\sqrt{2}A_{f_{2,1}}\frac{\mathrm{Re}(A'^{*}_{0}A'_{\perp})}{\sum_p |A'_p|^2}, \quad (34)$$

$$O_9(a_2) \equiv \left(\frac{d\Gamma}{da_2}\right)^{-1}\left(\int\limits_0^{\pi} d\varphi\frac{d^2\Gamma}{da_2 d\varphi} - \int\limits_{\pi}^{2\pi} d\varphi \ldots\right) =$$
$$= -\frac{9}{32}\sqrt{2}\pi A_{f_1}A_{f_2}\frac{\mathrm{Im}(A'^{*}_{0}A'_{\perp})}{\sum_p |A'_p|^2}. \quad (35)$$

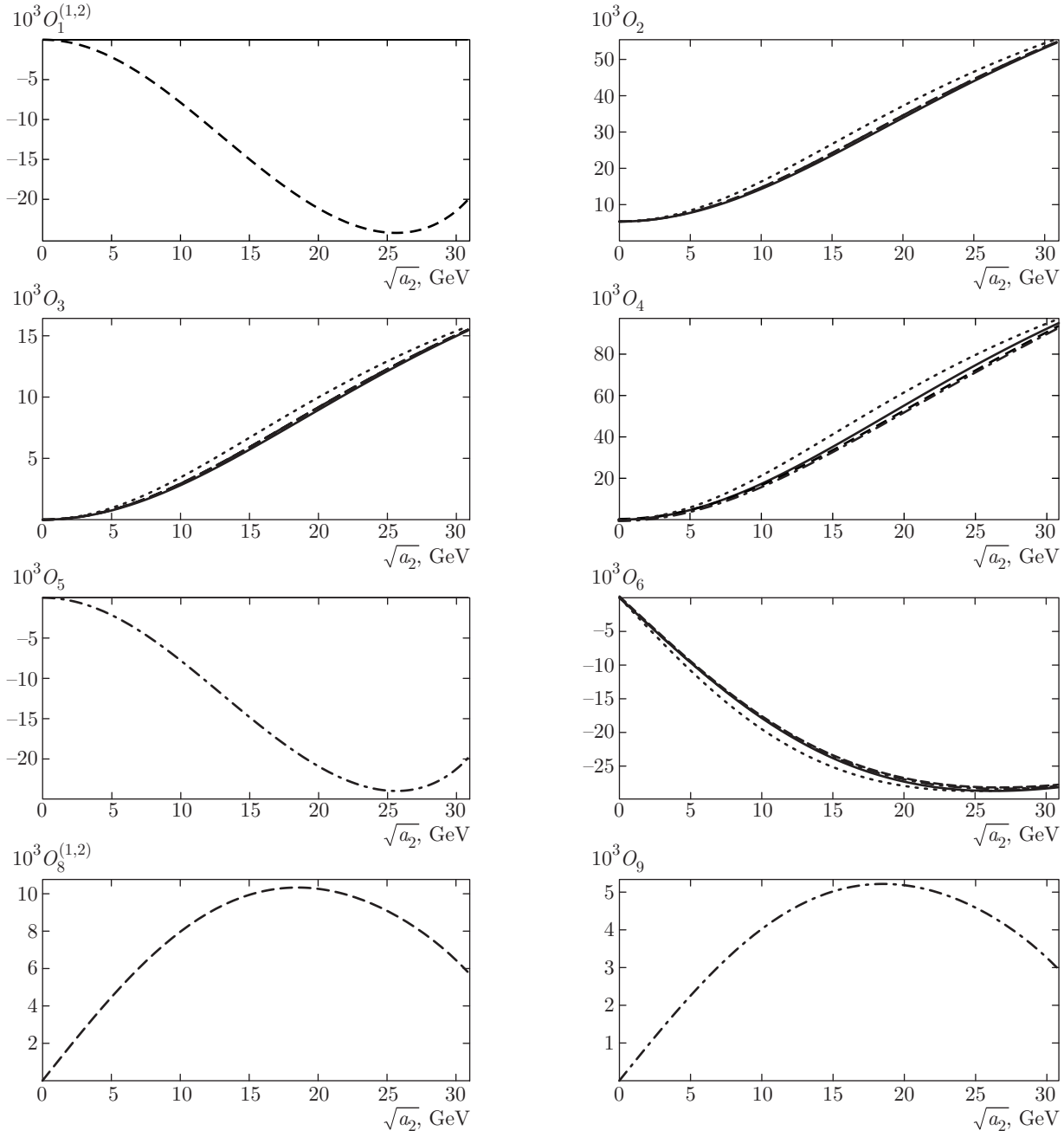

Fig. 4. The observables $O_1^{(1,2)}$, O_2 (at $\beta = 90°$, $\alpha = 70°$), O_3, O_4, O_5, O_6, $O_8^{(1,2)}$, and O_9 for the decay $h \to$ $\to Z_1^* Z_2^* \to l_1^- l_1^+ l_2^- l_2^+$ $(l_j = e, \mu, \tau,\ l_1 \neq l_2)$ as functions of $\sqrt{a_2}$ in the case $|a'_{hZ}| = 1$, $b'_{hZ} = 0$, $c'_{hZ} = 0$ (solid lines); $a'_{hZ} = 1$, $b'_{hZ} = 0$, $c'_{hZ} = 0.5$ (dashed lines); $a'_{hZ} = 1$, $b'_{hZ} = 0$, $c'_{hZ} = 0.5i$ (dash-dotted lines); and $a'_{hZ} = 1$, $b'_{hZ} = -0.5$, $c'_{hZ} = 0$ (dotted lines)

From the measured observables $O_i(a_2)$, we can obtain constraints on the dependences of the couplings $a'_Z(a_2)$, $b'_Z(a_2)$, and $c'_Z(a_2)$. As regards $O_2(a_2)$, it can be measured at a fixed value of $\sqrt{a_2}$ and at various values of the parameters β and α. Then, after obtaining central values and uncertainties of the quantity $|A'_0|^2/\sum_p |A'_p|^2$ from Eq. (28) at several sets of values of β and α, we can combine these central values and uncertainties and thereby obtain the value of $|A'_0|^2/\sum_p |A'_p|^2$ with greater precision than in the case of any particular values of β and α.

As an illustration of the behavior of these observables, in Fig. 4 we show their $\sqrt{a_2}$-dependence with the constant a'_{hZ}, b'_{hZ}, and c'_{hZ} from sets (24). The obser-

vable $O_2(a_2)$ is presented for $\beta = 90^\circ$ and $\alpha = 70^\circ$.

As we can see, for each of the observables $O_2(a_2)$, $O_3(a_2)$, $O_4(a_2)$, and $O_6(a_2)$ their dependences on $\sqrt{a_2}$ for all the four sets in (24) are very close. The observables $O_2(a_2)$ (at $\beta = 90^\circ$ and $\alpha = 70^\circ$) and $O_4(a_2)$ are relatively large with the maximum values greater than 0.05, and therefore measuring these observables requires a relatively small amount of data, while $O_3(a_2)$ and $O_6(a_2)$ are smaller, which complicates their experimental observation.

Further, $O_1^{(1,2)}(a_2)$, $O_5(a_2)$, $O_8^{(1,2)}(a_2)$, and $O_9(a_2)$ vanish for $c'_{hZ}(a_2) = 0$, according to Eqs. (27), (31), (34), and (35) and Fig. 4. Therefore, these observables can give significant constraints on the CP -odd coupling $c'_{hZ}(a_2)$, although their moduli are relatively small.

The functions $O_7^{(1,2)}(a_2)$ are proportional to $\mathrm{Im}(a'^*_{hZ}b'_{hZ})$ (see (33) and (6)), and, consequently, they are equal to zero for any set from (24). Among all the observables under consideration, $O_7^{(1,2)}(a_2)$ are the only ones vanishing in the case $b'_{hZ}(a_2) = 0$ for any $a'_{hZ}(a_2)$ and $c'_{hZ}(a_2)$. Therefore, knowing the dependences $O_7^{(1,2)}(a_2)$ allows obtaining appreciable constraints on the function $b'_{hZ}(a_2)$. However, in case (25), these observables turn out to be relatively small in absolute value (see Fig. 5).

We note that regardless of the values of the couplings $a'_Z(a_2)$, $b'_Z(a_2)$, and $c'_Z(a_2)$, it follows from (27)–(35) that for any a_2,

$$\begin{aligned}
&O_1^{(1,2)} \in \left[-\frac{3}{4}A_{f_{1,2}},\, \frac{3}{4}A_{f_{1,2}}\right], \quad O_2 \in [0,\, 1],\\
&O_3 \in \left[0,\, \frac{9}{16}A_{f_1}A_{f_2}\right], \quad O_4, O_5 \in \left[-\frac{1}{2\pi},\, \frac{1}{2\pi}\right],\\
&O_6, O_9 \in \left[-\frac{9}{64}\sqrt{2}\pi A_{f_1}A_{f_2},\, \frac{9}{64}\sqrt{2}\pi A_{f_1}A_{f_2}\right],\\
&O_7^{(1,2)}, O_8^{(1,2)} \in \left[-\frac{3}{16}\sqrt{2}A_{f_{2,1}},\, \frac{3}{16}\sqrt{2}A_{f_{2,1}}\right].
\end{aligned} \tag{36}$$

Since $A_{e^-} = A_{\mu^-} = A_{\tau^-} \approx 0.214$, $A_{\nu_e} = A_{\nu_\mu} = A_{\nu_\tau} = 1$, $A_u = A_c = A_t \approx 0.697$, and $A_d = A_s = A_b \approx 0.941$, the moduli of $O_1^{(1,2)}(a_2)$, $O_7^{(1,2)}(a_2)$, $O_8^{(1,2)}(a_2)$, $O_3(a_2)$, $O_6(a_2)$, and $O_9(a_2)$ for decays (1) with quarks and/or neutrinos in the final states are greater than those for decays (1) to leptons, and therefore the former processes seem more feasible for experimental study. On the other hand, detection of leptons is much easier. That is why the study of each decay channel of type (1) has advantages and disadvantages that strongly depend on the experimental methods and parameters of the detectors. Consequently, measuring the observables $O_1^{(1,2)}(a_2), \ldots, O_9(a_2)$ for various decay channels and for various invariant masses of the fermion pair ($\sqrt{a_2}$) may help impose constraints on the XZZ couplings $a'_Z(a_2)$, $b'_Z(a_2)$, and $c'_Z(a_2)$.

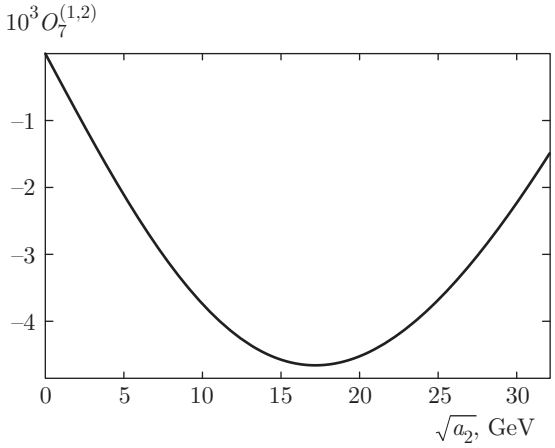

Fig. 5. The observables $O_7^{(1,2)}$ for the decay $h \to Z_1^* Z_2^* \to l_1^- l_1^+ l_2^- l_2^+$ ($l_j = e, \mu, \tau$, $l_1 \neq l_2$) versus $\sqrt{a_2}$ in the case $a'_{hZ} = 1$, $b'_{hZ} = -0.5i$, $c'_{hZ} = 0$

3. CONCLUSIONS

We have considered the decay of a neutral particle X with zero spin and arbitrary CP parity into two off-mass-shell Z bosons (Z_1^* and Z_2^*) each of which decays to a fermion–antifermion pair, i. e., the decay $X \to Z_1^* Z_2^* \to f_1\bar{f}_1 f_2\bar{f}_2$. This decay has been examined at the tree level for nonidentical fermions, $f_1 \neq f_2$. In the approximation of massless fermions, a formula for the fully differential width has been obtained. It has been established that the narrow-Z-width approximation is applicable to finding differential decay widths of $X \to Z_1^* Z_2^* \to f_1\bar{f}_1 f_2\bar{f}_2$ only if the invariant mass $\sqrt{a_2}$ of the pair $f_2\bar{f}_2$ lies in an interval $\left(0, m_X - \sqrt{m_Z^2 + \varepsilon_2}\right]$. If the parameter ε_2 becomes larger, the accuracy of the used approximation increases, but the interval in which the approximation is valid reduces. As an optimal value of ε_2, we have chosen $\varepsilon_2 = 3m_Z\Gamma_Z$.

In the narrow-Z-width approximation but without the neglect of Γ_Z in the propagator of Z_2^*, formulas for the total width of decay (1) and the total width of $h \to Z_1^* Z_2^*$ have been derived. The first formula is also valid in the case $f_1 = f_2$. We note that in Ref. [23], in the framework of the SM, the total width of decay $X \to ZZ^* \to Zf\bar{f}$ was found in the approximation $\Gamma_Z \approx 0$ in the propagator of Z^*. We can similarly obtain the total width of decay (1) in the SM with Γ_Z disregarded in the propagator of Z_2^*, but formula (A.2) derived in this paper is more general and more precise.

Using the CMS data [3], we have found constraints on the couplings a'_{hZ}, b'_{hZ}, and c'_{hZ}, which determine the hZZ interaction and the CP properties of the boson h detected in the experiments [1]. Comparing our constraints with those reported in Refs. [36,37], we note appreciable overlaps between the three results. Besides, we have derived the allowed interval for a ratio not studied in [36, 37]. Taking our allowed regions into account, we have selected several sets of values of the couplings q'_{hZ} $(q = a, b, c)$ and analyzed the results for these sets.

The observables $O_1^{(1,2)}(a_2), \ldots, O_9(a_2)$, measuring which will allow obtaining constraints on the dependences of q'_Z on $\sqrt{a_2}$, are defined. It is shown that the observables $O_1^{(1,2)}(a_2)$, $O_5(a_2)$, $O_8^{(1,2)}(a_2)$, and $O_9(a_2)$ vanish in the case $c'_Z(a_2) = 0$, and therefore their experimental dependences on $\sqrt{a_2}$ can impose significant constraints on the CP-odd coupling $c'_Z(a_2)$. The observables $O_7^{(1,2)}(a_2)$ vanish if $b'_Z(a_2) = 0$, and therefore their measurement is important for finding the CP-even coupling $b'_Z(a_2)$.

We note that the absolute values of $O_1^{(1,2)}(a_2)$, $O_7^{(1,2)}(a_2)$, $O_8^{(1,2)}(a_2)$, $O_3(a_2)$, $O_6(a_2)$, and $O_9(a_2)$ for decays (1) where f_1 and/or f_2 is a quark or a neutrino are greater than those for the processes in which the fermions are leptons. At the same time, the processes with the leptons are much more convenient from the experimental standpoint.

Thus, measurement of the observables $O_1^{(1,2)}(a_2), \ldots, O_9(a_2)$ for decays (1) can help clarify the CP properties of the particle X and the structure of the amplitude of the decay $X \to Z_1^* Z_2^*$.

The authors thank S. Ivashyn for the useful discussions. The work is supported in part by the National Academy of Sciences of Ukraine (project ЦО-15-1/2015) and the Ministry of Education and Science of Ukraine (project 0115U00473).

APPENDIX

Calculation of the total widths of the decays $X \to Z_1^* Z_2^* \to f_1\overline{f}_1 f_2\overline{f}_2$ and $h \to Z_1^* Z_2^*$

In this Appendix, we calculate the total width of the decay $X \to Z_1^* Z_2^* \to f_1\bar{f}_1 f_2\bar{f}_2$ for the m_X values such that $m_X > m_Z$ and for the dependences of $a_Z(a_1, a_2)$, $b_Z(a_1, a_2)$, and $c_Z(a_1, a_2)$ such that the differential width $d^2\Gamma/da_1 da_2$ has a sharp maximum when $\sqrt{a_1} = m_Z$ or $\sqrt{a_2} = m_Z$ and the functions $|a'_Z|$, $|b'_Z|$, $|c'_Z|$, and $\cos(\arg b'_Z - \arg a'_Z)$ ($q'_Z \equiv q_Z(m_Z^2, a_2)$; $q = a, b, c$) are independent of a_2. For example, $|a_Z| \approx \approx 1$, $b_Z \approx 0$, and $c_Z \approx 0$ are such dependences (see Sec. 2.2). Then we calculate the total decay width of $h \to Z_1^* Z_2^*$ and examine the applicability of the approximation $\Gamma_Z \approx 0$ to the derivation of the total widths.

1. The total width of the decay $X \to Z_1^* Z_2^* \to \to f_1\bar{f}_1 f_2\bar{f}_2$. Similarly to the derivation of Eq. (11), we find that

$$\Gamma \approx \frac{2\pi}{m_Z\Gamma_Z} \int\limits_0^{(m_X - m_Z)^2} da_2 f(m_Z^2, a_2). \qquad \text{(A.1)}$$

We consider the case where $|a'_Z|$, $|b'_Z|$, $|c'_Z|$, and $\cos(\arg b'_Z - \arg a'_Z)$ are independent of a_2. Having exactly calculated the integral in Eq. (A.1) with Eqs. (10) and (6) taken into account, we obtain

$$\Gamma \approx (a_{f_1}^2 + v_{f_1}^2)(a_{f_2}^2 + v_{f_2}^2) \times \times f_0(a'_Z, b'_Z, c'_Z, m_Z, \Gamma_Z, s), \qquad \text{(A.2)}$$

where

$$f_0(a'_Z, b'_Z, c'_Z, m_Z, \Gamma_Z, s) \equiv \frac{\sqrt{2}G_F^3 m_Z^7 m_X}{2^{10}3^3\pi^4\Gamma_Z} \times$$
$$\times \Bigg[(1-\alpha)\Big(-24(23\alpha-5)|a'_Z|^2 + (3\alpha^3 - 37\alpha^2 - \alpha(235+6\beta^2) + 77 - 54\beta^2)|b'_Z|^2 -$$
$$- 16(2\alpha^2 + 26\alpha - 13 + 3\beta^2)\,\mathrm{Re}(a'^*_Z b'_Z) + 64\alpha(\alpha^2 + 40\alpha - 11 + 6\beta^2)|c'_Z|^2\Big) + 6\ln\left(\frac{1}{\alpha}\right) \times$$
$$\times \Big(4(12\alpha^2 - 18\alpha + 3 - \beta^2)|a'_Z|^2 + (30\alpha^2 - 10\alpha(3-\beta^2) + 5 - 10\beta^2 + \beta^4)|b'_Z|^2 +$$
$$+ 8(6\alpha^2 - \alpha(9-\beta^2) + 2 - 2\beta^2)\,\mathrm{Re}(a'^*_Z b'_Z) - 32\alpha(6\alpha^2 - \alpha(9-\beta^2) + 1 - 3\beta^2)|c'_Z|^2\Big) +$$
$$+ s\frac{3\sqrt{2}}{\beta}\Bigg(P(\alpha, \beta, a'_Z, b'_Z, c'_Z, r_+, -4\beta r_-) \times$$

$$\times \ln \frac{(1-\alpha)^2\sqrt{(4\alpha-1+\beta^2)^2+4\beta^2}+(3\alpha-1)^2+\beta^2(\alpha+1)^2+s\sqrt{2}(1-\alpha)((3\alpha-1)r_- - \beta(\alpha+1)r_+)}{4\alpha(\alpha^2+\beta^2)} +$$
$$+ 2P(\alpha,\beta,a'_Z,b'_Z,c'_Z,r_-,4\beta r_+)\left(\pi - \arg\left(-\alpha(3\alpha-1+\beta^2)-\beta^2+s\frac{1-\alpha}{\sqrt{2}}(\beta r_+ - \alpha r_-) + \right.\right.$$
$$\left.\left. + i(1-\alpha)\left(s\frac{\alpha r_+ + \beta r_-}{\sqrt{2}} - \beta(1-\alpha)\right)\right)\right)\Bigg], \quad \text{(A.3)}$$

$$\alpha \equiv \left(\frac{m_Z}{m_X}\right)^2, \quad \beta \equiv \frac{m_Z\Gamma_Z}{m_X^2},$$

$$P(\alpha,\beta,a'_Z,b'_Z,c'_Z,x,y) \equiv 2(2x(12\alpha^2-4\alpha+1-\beta^2)+ + y(6\alpha-1))|a'_Z|^2 + (x(16\alpha^2-8\alpha(1-\beta^2)+1- - 6\beta^2+\beta^4)+y(4\alpha-1+\beta^2))|b'_Z|^2 + + (4x(8\alpha^2-2\alpha(3-\beta^2)+1-3\beta^2)+ + y(8\alpha-3+\beta^2))\,\mathrm{Re}(a'^*_Z b'_Z) - - 8\alpha(4x(4\alpha^2-\alpha(1-\beta^2)-2\beta^2)+ + y(6\alpha-1+\beta^2))|c'_Z|^2, \quad \text{(A.4)}$$

$$r_\pm \equiv \sqrt{\sqrt{(4\alpha-1+\beta^2)^2+4\beta^2} \pm (4\alpha-1+\beta^2)}. \quad \text{(A.5)}$$

In place of s, we can take 1 or -1:

$$f_0(a'_Z,b'_Z,c'_Z,m_Z,\Gamma_Z,-1) = f_0(a'_Z,b'_Z,c'_Z,m_Z,\Gamma_Z,1).$$

In this paper, the argument $\arg z$ of a complex number z is defined as

$$\arg z = \arctan\frac{\mathrm{Im}\,z}{\mathrm{Re}\,z} + \pi n(\mathrm{Re}\,z,\mathrm{Im}\,z) \quad \forall z \in C|\,\mathrm{Re}\,z \neq 0,$$
$$\arg z = \pi\left(\frac{1}{2} + \Theta(-\mathrm{Im}\,z)\right) \quad \forall z \in C|(\mathrm{Re}\,z = 0 \ \text{ and } \ \mathrm{Im}\,z \neq 0), \quad \text{(A.6)}$$

where $n(x,y) \equiv \Theta(-x) + 2\,\Theta(x)\Theta(-y) \ \ \forall x \neq 0$,

$$\Theta(x) \equiv 0 \ \ \forall x \in (-\infty, 0], \qquad \Theta(x) \equiv 1 \ \ \forall x \in (0, +\infty). \quad \text{(A.7)}$$

It follows from definition (A.6) that $\arg z$ is the angle measured clockwise on the complex plane from the vector $(\mathrm{Re}\,z, \mathrm{Im}\,z)$ toward the vector $(1,\,0)$ and $\arg z \in \in [0, 2\pi)$. Sometimes, a different function

$$\arg' z \equiv \arg z - 2\pi\Theta(-\mathrm{Im}\,z) \quad \text{(A.8)}$$

is used as the argument of z in the literature. It follows from (A.8) that $\arg' z \in (-\pi, \pi]$. We note that we have already used $\arg z$ above in the expression $\cos(\arg b_Z - \arg a_Z)$, but because

$$\cos(\arg b_Z - \arg a_Z) = \cos(\arg' b_Z - \arg' a_Z),$$

the distinction between $\arg z$ and $\arg' z$ was irrelevant at that point.

Calculating the integral over a_2 in Eq. (A.1), we find an antiderivative of $f(m_Z^2, a_2)$ on the interval $[0, (m_X - m_Z)^2]$. In this antiderivative, the function $\arg u_1(a_2)$ naturally appears, where $u_1(a_2)$ is a complex-valued dimensionless function such that

$$\forall a_2 \in [0, (m_X - m_Z)^2) \quad \mathrm{Im}\,u_1(a_2) \neq 0,$$
$$\mathrm{Im}\,u_1((m_X - m_Z)^2) = 0,$$
$$\mathrm{Re}\,u_1((m_X - m_Z)^2) < 0. \quad \text{(A.9)}$$

Here, $\arg' u_1(a_2)$ does not emerge in place of $\arg u_1(a_2)$ since, according to (A.8), the function $\arg' z$ has a discontinuity on the half-line $\mathrm{Im}\,z = 0$, $\mathrm{Re}\,z < 0$ and therefore $\arg' u_1(a_2)$ has a discontinuity at the point $a_2 = (m_X - m_Z)^2$. To avoid this drawback, it is convenient to use $\arg z$ in Eq. (A.3).

We note that in the case of the Higgs boson, i. e., $X = h$, Eq. (A.3) can also be written in terms of the function $\arg'$: for this, we have to substitute $\pi - \arg\ldots$ by $s\pi - \arg'\ldots$ in Eq. (A.3), since according to (A.8) and to the data in Table 1, $\pi - \arg\ldots = s\pi - \arg'\ldots$

In the case of identical fermions, $f_1 = f_2$, we can neglect the interference term and then in order to obtain a formula for Γ, we have to multiply the right-hand side of relation (A.2) by $1/(2!2!)$ (in view of the identity of the final fermions) and by 2 (because the contribution of the diagram with the permutation of particles to Γ is equal to that of the diagram without the permutation), i. e., to multiply the right-hand side by $1/2$. Consequently, for any f_1 and f_2,

$$\Gamma \approx \left(1 - \frac{1}{2}\delta_{f_1 f_2}\right)(a_{f_1}^2 + v_{f_1}^2)(a_{f_2}^2 + v_{f_2}^2) \times \times f_0(a'_Z,b'_Z,c'_Z,m_Z,\Gamma_Z,s) \equiv \Gamma_{\Gamma_Z}, \quad \text{(A.10)}$$

where $\delta_{f_1 f_2} \equiv 0\,(1)$ at $f_1 \neq f_2$ ($f_1 = f_2$). The neglected interference term seems to be small based on qualitative arguments in Ref. [38]. For a quantitative estimate, we can use Ref. [30] (see Table 1 there), according to which the interference contribution to $\Gamma(h \to Z_1^* Z_2^* \to 4e)$ in the SM at the tree level is 5.80 % for $m_h = 140$ GeV.

In Ref. [23], the width of the decay $h \to ZZ^* \to Zf\bar{f}$ was derived at the tree level in the SM with Γ_Z neglected in the propagator of Z^*. Following [23], when calculating the integral in Eq. (A.1), we can also neglect Γ_Z in the expression for $f(m_Z^2, a_2)$, and then we obtain the following approximate formula for Γ in the SM:

$$\Gamma|_{SM} \approx \left(1 - \frac{1}{2}\delta_{f_1 f_2}\right) \frac{\sqrt{2} G_F^3 m_Z^7 m_X}{2^7 3^2 \pi^4 \Gamma_Z} \times \\ \times (a_{f_1}^2 + v_{f_1}^2)(a_{f_2}^2 + v_{f_2}^2) \times \\ \times \left(6 \frac{1 - 8\alpha + 20\alpha^2}{\sqrt{4\alpha - 1}} \arccos \frac{3\alpha - 1}{2\alpha^{3/2}} - \frac{1 - \alpha}{\alpha} \times \right. \\ \left. \times (2 - 13\alpha + 47\alpha^2) + 3(1 - 6\alpha + 4\alpha^2) \ln \frac{1}{\alpha}\right) \equiv \\ \equiv \Gamma_0|_{SM}. \quad \text{(A.11)}$$

It follows from (A.11) and (A.10) that at $m_X = m_h$,

$$\Gamma_0|_{SM} \approx 1.001 \Gamma_{\Gamma_Z}|_{SM}. \quad \text{(A.12)}$$

Besides, $\Gamma_0 > \Gamma_{\Gamma_Z}$ (for any a'_Z, b'_Z, c'_Z, f_1, and f_2) because when deriving the formula for Γ_0, we neglect the width Γ_Z in $f(m_Z^2, a_2)$ and the value of the integral increases. Still, according to (A.12), the difference between $\Gamma_0|_{SM}$ and $\Gamma_{\Gamma_Z}|_{SM}$ is about one per mille.

Finally, we note that at $m_X = m_h$ we can represent the dependence of the function f_0 on the XZZ couplings a'_Z, b'_Z, and c'_Z in the convenient form

$$f_0(a'_Z, b'_Z, c'_Z, m_Z, \Gamma_Z, s) \approx \left(3.359|a'_Z|^2 + 0.052|b'_Z|^2 + \right. \\ \left. + 0.594\,\mathrm{Re}(a'^*_Z b'_Z) + 0.125|c'_Z|^2\right) \text{ keV}. \quad \text{(A.13)}$$

2. The total width of the decay $h \to Z_1^* Z_2^*$. The total decay width $\Gamma(h \to Z_1^* Z_2^*)$ is

$$\Gamma(h \to Z_1^* Z_2^*) = \sum_{f_1} \sum_{f_2 \geq f_1} \Gamma|_{m_X = m_h}, \quad \text{(A.14)}$$

where the sums run over the fermions e^-, μ^-, τ^-, ν_e, ν_μ, ν_τ, u_i, c_i, d_i, s_i, b_i (because $m_h \in (4m_b, 2m_t]$), and $i = r, g, b$ is an index of quark color. It follows from Eqs. (A.14) and (A.12) that in the SM,

$$\Gamma_0(h \to Z_1^* Z_2^*) \approx 1.001 \Gamma_{\Gamma_Z}(h \to Z_1^* Z_2^*). \quad \text{(A.15)}$$

We use Eq. (A.10) in what follows because it is more precise than Eq. (A.11) and consider the case where $|a'_{hZ}|$, $|b'_{hZ}|$, $|c'_{hZ}|$, and $\cos(\arg b'_{hZ} - \arg a'_{hZ})$ do not depend on a_2. From Eqs. (A.14), (A.10), and (A.3) we then derive that

$$\Gamma(h \to Z_1^* Z_2^*) \approx f_0(a'_{hZ}, b'_{hZ}, c'_{hZ}, m_Z, \Gamma_Z, s)|_{m_X = m_h} \times \\ \times \left(\frac{1}{2}\sum_{f_1}(a_{f_1}^2 + v_{f_1}^2)^2 + \right. \\ \left. + \frac{1}{2}\sum_{f_1}\sum_{f_2 \neq f_1}(a_{f_1}^2 + v_{f_1}^2)(a_{f_2}^2 + v_{f_2}^2)\right) = \\ = \frac{f_0(\ldots)}{2}\left(\sum_f (a_f^2 + v_f^2)\right)^2 = \frac{f_0(\ldots)}{18} \times \\ \times \left(\frac{103}{2} - 100\left(\frac{m_W}{m_Z}\right)^2 + 80\left(\frac{m_W}{m_Z}\right)^4\right)^2. \quad \text{(A.16)}$$

Calculating, we find the total decay width for sets (24) and (25):

$$\begin{aligned} &|a'_{hZ}| = 1, \quad b'_{hZ} = 0, \\ &c'_{hZ} = 0 \Rightarrow \Gamma(h \to Z_1^* Z_2^*) \approx \\ &\qquad \approx 91.16^{+16.66}_{-14.50} \text{ keV}, \\ &|a'_{hZ}| = 1, \quad b'_{hZ} = 0, \\ &|c'_{hZ}| = 0.5 \Rightarrow \Gamma(h \to Z_1^* Z_2^*) \approx \\ &\qquad \approx 92.01^{+16.85}_{-14.67} \text{ keV}, \\ &a'_{hZ} = 1, \quad b'_{hZ} = -0.5, \\ &c'_{hZ} = 0 \Rightarrow \Gamma(h \to Z_1^* Z_2^*) \approx \\ &\qquad \approx 83.45^{+15.06}_{-13.14} \text{ keV}, \\ &a'_{hZ} = 1, \quad b'_{hZ} = \pm 0.5i, \\ &c'_{hZ} = 0 \Rightarrow \Gamma(h \to Z_1^* Z_2^*) \approx \\ &\qquad \approx 91.51^{+16.74}_{-14.57} \text{ keV}. \end{aligned} \quad \text{(A.17)}$$

The uncertainties shown in Eqs. (A.17) are calculated by finding the maximum and minimum values of $\Gamma(h \to Z_1^* Z_2^*)$ in the region $v \in [v_0 - 3\sigma_v, v_0 + 3\sigma_v]$ ($v = G_F, m_h, m_Z, m_W, \Gamma_Z$). Here, v_0 is the central value of a quantity v, and σ_v is the 1-standard-deviation uncertainty of v; according to the data in Table 1, $G_{F0} = 1.1663787 \cdot 10^{-5}$ GeV^{-2}, $\sigma_{G_F} = 6 \cdot 10^{-12}$ GeV^{-2}, $m_{h0} = 125.7$ GeV, $\sigma_{m_h} = 0.4$ GeV, etc.

REFERENCES

1. G. Aad et al. (ATLAS Collaboration), Phys. Lett. B **716**, 1 (2012); S. Chatrchyan et al. (CMS Collaboration), Phys. Lett. B **716**, 30 (2012).

2. G. Aad et al. (ATLAS Collaboration), Phys. Lett. B **726**, 88 (2013).

3. S. Chatrchyan et al. (CMS Collaboration), Phys. Rev. D **89**, 092007 (2014).

4. S. Chatrchyan et al. (CMS Collaboration), Phys. Rev. Lett. **110**, 081803 (2013).

5. A. Pilaftsis and C. E. M. Wagner, Nucl. Phys. B **553**, 3 (1999).

6. V. Barger, P. Langacker, M. McCaskey et al., Phys. Rev. D **79**, 015018 (2009).

7. G. C. Branco, P. M. Ferreira, L. Lavoura et al., Phys. Rep. **516**, 1 (2012).

8. D. Bailin and A. Love, *Cosmology in Gauge Field Theory and String Theory*, Institute of Physics Publ., Bristol–Philadelphia (2004).

9. M. B. Voloshin, Phys. Rev. D **86**, 093016 (2012).

10. F. Bishara, Y. Grossman, R. Harnik et al., JHEP **1404**, 084 (2014).

11. A. Yu. Korchin and V. A. Kovalchuk, Phys. Rev. D **88**, 036009 (2013); A. Yu. Korchin and V. A. Kovalchuk, Acta Phys. Polon. B **44**, 2121 (2013).

12. J. S. Gainer, W. Y. Keung, I. Low, and P. Schwaller, Phys. Rev. D **86**, 033010 (2012).

13. A. Y. Korchin and V. A. Kovalchuk, Eur. Phys. J. C **74**, 3141 (2014).

14. S. Y. Choi, D. J. Miller, M. M. Mühlleitner et al., Phys. Lett. B **553**, 61 (2003).

15. V. A. Kovalchuk, Zh. Eksp. Teor. Fiz. **134**, 907 (2008) [JETP **107**, 774 (2008)].

16. A. Menon, T. Modak, D. Sahoo et al., Phys. Rev. D **89**, 095021 (2014).

17. Y. Sun, X.-F. Wang, and D.-N. Gao, Int. J. Mod. Phys. A **29**, 1450086 (2014).

18. A. De Rujula, J. Lykken, M. Pierini et al., Phys. Rev. D **82**, 013003 (2010); Y. Gao, A. V. Gritsan, Z. Guo et al., Phys. Rev. D **81**, 075022 (2010); S. Bolognesi, Y. Gao, A. V. Gritsan et al., Phys. Rev. D **86**, 095031 (2012); D. Stolarski and R. Vega-Morales, Phys. Rev. D **86**, 117504 (2012); P. Avery, D. Bourilkov, M. Chen et al., Phys. Rev. D **87**, 055006 (2013); M. Chen, T. Cheng, J. S. Gainer et al., Phys. Rev. D **89**, 034002 (2014); B. Bhattacherjee, T. Modak, S. K. Patra et al., arXiv:1503.08924 [hep-ph].

19. M. Gasperini, Phys. Lett. B **327**, 214 (1994).

20. Z. Chacko, R. Franceschini, and R. K. Mishra, JHEP **1304**, 015 (2013).

21. B. Bellazzini, C. Csáki, J. Hubisz et al., Eur. Phys. J. C **73**, 2333 (2013).

22. J. Serra, EPJ Web Conf. **60**, 17005 (2013).

23. W.-Y. Keung and W. J. Marciano, Phys. Rev. D **30**, 248 (1984).

24. R. M. Godbole, D. J. Miller, and M. M. Mühlleitner, JHEP **0712**, 031 (2007).

25. W.-Y. Keung, I. Low, and J. Shu, Phys. Rev. Lett. **101**, 091802 (2008); T. L. Trueman, Phys. Rev. D **18**, 3423 (1978); J. R. Dell'Aquila and C. A. Nelson, Phys. Rev. D **33**, 80 (1986).

26. K. A. Olive et al. (Particle Data Group), Chin. Phys. C **38**, 090001 (2014).

27. N. N. Achasov and V. V. Gubin, Pisma v Zh. Eksp. Teor. Fiz. **62**, 182 (1995) [JETP Lett. **62**, 191 (1995)].

28. D. Berdine, N. Kauer, and D. Rainwater, Phys. Rev. Lett. **99**, 111601 (2007).

29. C. F. Uhlemann and N. Kauer, Nucl. Phys. B **814**, 195 (2009).

30. A. Bredenstein, A. Denner, S. Dittmaier, and M. M. Weber, Phys. Rev. D **74**, 013004 (2006).

31. G. Aad et al. (ATLAS Collaboration), arXiv:1504.05833 [hep-ex].

32. LHC Higgs Cross Section Working Group, https://twiki.cern.ch/twiki/bin/view/LH CP hysics/CERN YellowReportPageAt8TeV.

33. V. Khachatryan et al. (CMS Collaboration), Phys. Lett. B **736**, 64 (2014).

34. S. Heinemeyer et al. (LHC Higgs Cross Section Working Group), arXiv:1307.1347v2 [hep-ph].

35. J. S. Gainer, J. Lykken, K. T. Matchev et al., Phys. Rev. Lett. **111**, 041801 (2013).

36. V. Khachatryan et al. (CMS Collaboration), Phys. Rev. D **92**, 012004 (2015).

37. G. Aad et al. (ATLAS Collaboration), arXiv:1506.05669v1 [hep-ex].

38. J. C. Romão and S. Andringa, Eur. Phys. J. C **7**, 631 (1999).